# Quantifying and specifying the solar influence on terrestrial surface temperature

C. de Jager [a,*], S. Duhau [b], B. van Geel [c]

[a] Royal Netherlands Institute for Sea Research, P.O. Box 59, 1790 AB Den Burg, The Netherlands
[b] Departamento de Física, Facultad de Ciencias Exactas y Naturales, Universidad de Buenos Aires, 1428 Buenos Aires, Argentina
[c] Institute for Biodiversity and Ecosystem Dynamics, Research Group Paleoecology and Landscape Ecology, Faculty of Science, University of Amsterdam, P.O. Box 94248, 1090 GE Amsterdam, The Netherlands

## ARTICLE INFO

## ABSTRACT

This investigation is a follow-up of a paper in which we showed that both major magnetic components of the solar dynamo, viz. the toroidal and the poloidal ones, are correlated with average terrestrial surface temperatures. Here, we quantify, improve and specify that result and search for their causes.

We studied seven recent temperature files. They were smoothed in order to eliminate the Schwabe-type (11 years) variations. While the total temperature gradient over the period of investigation (1610–1970) is 0.087 °C/century; a gradient of 0.077 °C/century is correlated with the equatorial (toroidal) magnetic field component. Half of it is explained by the increase of the Total Solar Irradiance over the period of investigation, while the other half is due to feedback by evaporated water vapour. A yet unexplained gradient of −0.040 °C/century is correlated with the polar (poloidal) magnetic field. The residual temperature increase over that period, not correlated with solar variability, is 0.051 °C/century. It is ascribed to climatologic forcings and internal modes of variation.

We used these results to study present terrestrial surface warming. By subtracting the above-mentioned components from the observed temperatures we found a residual excess of 0.31° in 1999, this being the triangularly weighted residual over the period 1990–2008.

We show that solar forcing of the ground temperature associated with significant feedback is a regularly occurring feature, by describing some well observed events during the Holocene.

## 1. Introduction

In a previous paper (De Jager and Duhau, 2009b) we discussed the relationship between solar activity and average terrestrial surface temperature. A refinement, as compared to earlier investigations of that problem, was that we did not only deal with the correlation of terrestrial surface temperature with the manifestations of the solar toroidal magnetic field component, such as sunspots, the UV radiation emitted by the facular fields, solar flares and CMEs, but that we also considered the possible influence of the poloidal fields. The rationale behind that approach is that the two magnetic field components of the solar dynamo, viz. the toroidal and the poloidal ones, are comparable in magnetic flux. Hence there is no a priori reason for concentrating on only one of them when studying the possible solar influence on tropospheric temperatures.

On the basis of a study of seven temperature data files we found (De Jager and Duhau, 2009b) that the influence of the poloidal fields cannot be neglected. It was at that time reconstructed to amount to some 30% of that of the toroidal field component. The question which manifestation(s) of solar activity should be put responsible for the sun–troposphere connection was not touched.

We have since been involved in a more detailed recalculation of these results for various reasons: First, we got new aa-data. Next we also realized that the use of aa-data for the period 1610–1844, being based on extrapolated sunspot numbers could give rise to wrong results. The approach followed in that paper was based on a method comparable to our 'first attempt', described in Section 2. In that section we will show that this approach yields inaccurate results. Finally we thankfully acknowledge the receipt before publication of a critical paper by Komen (preprint). The outcome of the new study is part of the present paper. Later in this paper we explain the difference with the former results.

In our attempt to identify a solar agency we took into account that the solar variability has several components. Best known are the Schwabe and Hale cycles of ~11 and ~22 years, the

Gleissberg cycle of ~88 years, the De Vries cycle of 205 years, the Hallstatt cycle of ~2300 years (cf. review by De Jager, 2005). Most of these cycles, though, are not constant as some of them, notably the Schwabe and Hale cycles and particularly the Gleissberg cycle vary in length as well as in their time-dependent structure. It seems likely that each of the various components of these cycles may be associated with another solar physical mechanism, which has to be identified. Each of these may or may not be correlated with terrestrial surface temperatures and they may act differently. It is the purpose of this paper also to deal with that problem, in an attempt to identify the solar cycles that contribute to tropospheric warming.

To illustrate the problem we show in Fig. 1 the variation of the temperature with time since 1620. The data file is that of Moberg et al. (2005) extended after 1980 by that of Brohan et al. (2006) and Kennedy et al. (2008). The data have been smoothed with a procedure described by De Jager and Usoskin (2006), which consist in weighing the data with triangularly distributed weights over a time interval of plus and minus 9 years around the central date. Data smoothing is essential for the present problem because the notion 'climate' implies the study of terrestrial surface temperatures.

A gradual increase, with a gradient of 0.17° per century, is apparent in the diagram but we notice a change in the gradient after about 1790–1800. Also clear is the still steeper increase after 1970. Roughly one may distinguish between three periods, each with a different gradient $dT(t)/dt$: 1610–1800, 1800–1970 and after 1970.

The average secular temperature gradient of the Moberg–Brohan–Kennedy data, being $dT/dt = 0.17°$ per century, is not typical. All seven temperature data sets that are studied in this paper (cf. the references in Section 2) show a secular increase of temperature. The average value over the seven data sets is 0.087° per century. In these temperature data sets the lowest value, 0.036° per century, is for the data of Mann et al. (1999).

In the present paper we want to study the solar influence on the Earth's lower troposphere and notably on the surface temperature. In this introductory section we briefly summarize results from other authors that found correlation between solar activity and physical parameters of the troposphere, notably the ground temperatures. Coughlin and Tung (2004) found an 11-year sun-correlated signal in the lower troposphere. Usoskin et al. (2004b, 2004c) studied the correlation between solar activity and surface temperature over the last 1150 years and found a correlation coefficient of 0.7–0.8 with a significance level ranging between 94% and 98%. De Jager and Usoskin (2006) studied the correlation between the Moberg et al. temperatures and the Group Sunspot Number for the period 1620–1960. Their diagram (their Fig. 3) shows significant correlation, the correlation coefficient being 0.77 (+0.10/−0.17) with a significance level of 99.8%. Scafetta (2009) found a significant solar contribution in the
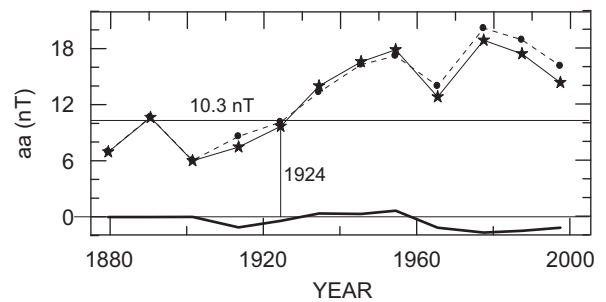


**Fig. 2.** The homogeneous (Lockwood, stars and thin solid line) and the standard (Mayaud; points, dotted line) aa geomagnetic index time series and the difference between both (thick line). The straight line at the 10.3 nT level indicates the ordinate of the Transition Point (TP). In 1924 the amplitude of the polar cycle was very near to the Transition Point value.

period before 1980. Le Mouël et al. (2008, 2009) detected a good correlation between some aspects of earth temperature variation and solar variability. According to Benestadt and Schmidt (2009) the sun contributed for 7% to the temperature increase in the 20th century while its contribution is negligible since 1980. Usoskin et al. (in press) found significant, though geographically separated solar effects on tropospheric ionisation.

Next, we describe the proxies used here. Following usual practice, the time series of sunspot cycle maxima $R_{max}$ and of the minima of the geomagnetic index $aa_{min}$ have been used as proxies for the amplitude modulation of the solar dynamo magnetic field in the toroidal and poloidal components, respectively. This is done because direct observations of the two field components are only available for the past few solar cycles. For the aa index we used the Mayaud (1975) data as recently corrected by Lockwood et al. (submitted for publication). The difference between these two data sets is shown in Fig. 2. These differences appear to be relatively small, but since the $R_{max}$ and the $aa_{min}$ data are correlated to a large extent, these small differences may result in large differences in the outcome of investigations, like the present one, that are based on a least squares treatment of four variables. We recall that at phase transitions between Grand Episodes the values of $aa_{min}$ and $R_{max}$ assume unique values, of 93.4 sunspot numbers and 10.34 nT, respectively (Duhau and De Jager, 2008). These co-ordinates identify the so-called Transition Point. The upper horizontal line in Fig. 2 at 1924 is drawn at that value. The vertical line in Fig. 2 at 93.4 is drawn at the Transition Point value for $R_{max}$. The $aa_{min}$ curve crossed the 1924 line during the phase transition of 1923–1924.

## 2. A reanalysis of the sun–climate connection

We investigate the relation between the annually averaged terrestrial surface temperature $T$ and the toroidal and poloidal fields. Observations (Fig. 1) show that $T$ increased gradually from the Maunder Minimum till the 20th century Grand Maximum. The same applies to $R_{max}$ as indicated by De Jager and Duhau (2009b; cf. their Figs. 2 and 1). It also applies to $aa_{min}$ (Fig. 3 of De Jager and Duhau, 2009b). Assuming these relationships to be linear, which is the simplest assumption in the absence of a physical theory, we write:

$$T = xR_{max} + y\, aa_{min} + z\, time + const \tag{1}$$

Here, the $z$-term is introduced to represent an assumed gradual rise of temperature with time that is not correlated with solar variability and that might be due to climatologic phenomena. With Eq. (1) we wish to determine the constants $x$, $y$ and $z$ in such a way that the resulting fit follows the interdecadal
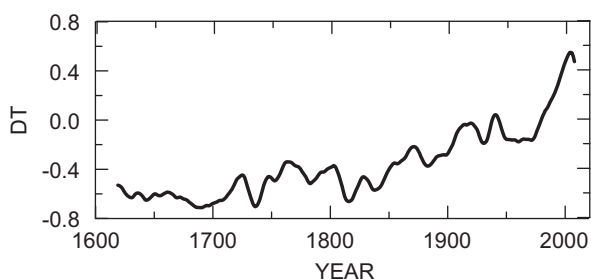


**Fig. 1.** Smoothed average terrestrial surface temperatures according to Moberg et al. (2005). Data from Brohan et al. (2006) and Kennedy et al. (2008), from 1980 onward are pasted to it.

variations, and we investigate how much of the secular $T$ rise can be accounted for. In this investigation we use the normalized values of $R_{max}$ and $aa_{min}$ to facilitate the calculations. Hence, the units of $x$ and $y$ are °C, while that of $z$ is chosen as °C/century.

The way of normalizing needs some discussion. In De Jager and Duhau (2009b) we normalized to the average values of $R_{max}$ and $aa_{min}$ over the time interval considered, which is admittedly an arbitrary approach, because any other time interval would give other normalization constants. In the present investigation we normalize to the Transition Point coordinates in the phase diagram (Duhau and De Jager, 2008). As elaborated in that paper, these coordinates are based on the theory of deterministic chaos (Weiss, 1987; Feynman and Gabriel, 1990; Weiss and Tobias, 2006; De Jager, 2005), as well as on an observational analysis of the nonlinear character of the solar dynamo and of its chaotic elements that characterise solar activity (Kremliovsky, 1995; Weiss and Tobias, 2006). We therefore claim that the normalization is physically justified and unique. But here we have to add that the way of normalizing does not affect the end result. If, for example, the normalizing constants would be multiplied by factors $p$ and $q$, then we would find that the resulting $x$ and $y$ values will appear to have been multiplied by the same factors and the functions $T_x = x.R_{max}$ and $T_y = y\,aa_{min}$ would remain the same. Also the resulting value of $z$ would not change. But the choice of the normalization is important for another reason: the ratio $y/x$ describes the relative contributions of the poloidal and the toroidal field components. This ratio depends on the normalization. The appropriate normalization for this aim is the one based on the Transition Point coordinates. This is further discussed in Section 4.

The investigation was applied to the seven temperature data sets that were used previously by De Jager and Usoskin (2006) and De Jager and Duhau (2009b). These are, numbered from 1 to 7: Moberg et al. (2005), Jones et al. (1998a, b), Mann et al. (1999), Briffa (2000), Overpeck et al. (1997), Crowley and Lowery (2000) and Mann and Jones (2003). It is well-known that the various published temperature reconstructions are fairly inhomogeneous. Not all of the above temperature data sets are really global. Some of them are restricted to certain global zones. In view of these apparent inhomogeneities it is difficult to select the 'best' or the 'most suitable' temperature file. We decided to choose all recent (i.e. after 1998) temperature files that are published in peer-refereed papers in international journals.

We want to determine $x$, $y$ and $z$, and their mean errors by least squares. The direct analysis leads to difficulties for various reasons as mentioned: the correlation of $R_{max}$ and $aa_{min}$ and the fact that, while $R_{max}$ is known for the period after 1610, direct observations of $aa_{min}$ are only known from 1844 onward.

A *first attempt*, being a least-squares analysis of the data in the restricted time interval 1844–1970 failed. The resulting r.m.s. errors of $x$, $y$, $z$ and *const* appear to be large enough to distrust the derived values.

In a *second attempt* we tried to solve Eq. (1) for the larger time interval 1610–1970. We tried to overcome the difficulty that $aa$-data are only available from 1844 onward by using the extrapolated $aa$-data of Nagovitsyn (2005, 2006, 2007). The weakness of this approach is that the extrapolation is partly based on sunspot numbers.

By least squares we solved $x$, $y$, $z$ and *const* from Eq. (1) for the time interval 1619–1970 hence yielding 352 equations with four unknowns. Although sunspot data are available from 1610 onward, the first 9 years are numerically omitted because of the smoothing procedure. The data had been smoothed by a triangular smoothing function with a base width of 18 years, as described in De Jager and Usoskin (2006). For the ending year we choose 1970, because there are indications of significant

antropogenic warming after about 1980. We note in this connection that Le Mouël et al. (2005) find that antropogenic warming only started to become dominant in the last decade of the 20th century. Hence our choice of 1970 seems a safe ending year.

We thus got 7 sets of data and their r.m.s. errors for the unknowns, these resulting from the seven temperature data sets; see Table 1a. The results show considerable scattering and large mean errors. After having found $x$, $y$ and $z$ we studied the $T(t)$ gradients for the original data sets, where $t$ is time. This was done by the least squares technique leading to the value $z_0 = dT/dt$. Here, $z_0$ is the total temperature gradient over the period studied, while $z$ is the gradient that results after subtraction of the sun-correlated part. The values of $(z_0 - z)/z_0$ then describe the relative contribution of sun-correlated warming to the gradual temperature increase over the period of 3.5 centuries that was investigated.

The weighted averages of the results, weighted according to the inverse squared mean errors are:
$\langle x \rangle = 0.1117 \pm 0.0092$; $\langle y \rangle = -0.0359 \pm 0.0096$;
hence $y/x = -0.321$.
$\langle z_0 \rangle = 0.0825 \pm 0.0057$ and $\langle z \rangle = 0.0671 \pm 0.0062$;
$\langle (z_0 - z)/z_0 \rangle = 0.2348 \pm 0.0250$.
Further: $(\langle z_0 \rangle - \langle z \rangle)/\langle z_0 \rangle = 0.1867$.

Although this attempt resulted in numerical data with a slightly better degree of accuracy than was found in the *first attempt* it is clear that the approach is too primitive. That can be judged from a glance at the ratio between the average (one sigma) r.m.s. errors and the average values of $x$ and $y$. The averages, as derived from Table 1a, are $\langle \mu_x \rangle / \langle x \rangle = 0.40$ and $\langle \mu_y \rangle / \langle y \rangle = 1.04$. It follows that the $x$-values are barely significant while the $y$ values are not at all. Therefore these results are just given as an illustration of the inherent numerical difficulties of the present problem. The main reason for presenting them here is to allow for a comparison with results from the following *third attempt*.

In that attempt we tried to overcome the difficulties of the first two attempts by working in two steps, and according to two different and, in a sense, opposite approaches.

In our first step we write

$$T = xR_{max} + const$$

hence neglecting for the time being the $y$ and $z$ terms, and we determined $x$ by least squares for the period for which sunspot data are available: 1619–1970. Thereafter we determined $y$ and *const* for data covering the period 1844–1970, by a least squares analysis of

$$T - xR_{max} = y\,aa_{min} + const$$

Having thus found $x$ and $y$ in the first approximation we tried to improve them by successive iterations, repeating the procedure for the residuals. It turned out that two iteration steps were as a rule sufficient. More iteration steps did not improve the results but they did increase the resulting mean errors.

**Table 1a**
Values of $x$, $y$, $z_0$ and $z$ and their r.m.s. errors ($\mu$) for the seven temperature files.

| T-file | x | $\mu_x$ | y | $\mu_y$ | $z_0$ | z | $\mu_z$ |
|---|---|---|---|---|---|---|---|
| 1 | .2359 | .0718 | −.0389 | .0607 | .0788 | .0575 | .0095 |
| 2 | .0751 | .0463 | −.0088 | .0348 | .0733 | .0588 | .0091 |
| 3 | .0465 | .0443 | −.0468 | .0368 | .0360 | .0147 | .0087 |
| 4 | .0841 | .0355 | −.0169 | .0293 | .0848 | .0709 | .0070 |
| 5 | .1513 | .0399 | −.0923 | .0331 | .0766 | .0650 | .0078 |
| 6 | .1957 | .0424 | −.1413 | .0352 | .1604 | .1505 | .0083 |
| 7 | .0831 | .0352 | −.0019 | .0311 | .0652 | .0474 | .0074 |

In the second step we went the other way round by first determining $y$ from

$$T = y\, aa_{min} + const$$

We did this for the period for which $aa$-data are available: 1844–1970. Thereafter $x$ was determined, similarly and complimentary to the above treatment.

The results from the two ways of analysis lead to similar results, with considerable scatter. After having found $x$ and $y$ we studied the $T(t)$ gradient, where $t$ is time. This was first done for the original $T$-data, leading to the value $z_0 = dT/dt$. Thereafter the gradient was determined for the residuals, hence describing the non-sun related temperature increase, leading to the gradient $z$ of the residual temperatures. This was also done by a least squares technique. The values of $(z_0-z)/z_0$ then describe the relative contribution of sun-correlated warming to the gradual temperature increase over the period of 3.5 centuries that was investigated.

We thus got 14 sets of data and their r.m.s. errors for the unknowns, these resulting from the seven temperature data sets and the two approaches. The numerical data are presented in Table 1b.

The weighted averages of the results, weighted according to the inverse squared mean errors are $\langle x \rangle = 0.3595 \pm 0.0071$ and $\langle y \rangle = -0.1851 \pm 0.0086$. Hence $y/x = -0.5194$. We again judge the accuracy of the data by deriving the ratios of average values $\langle \mu_x \rangle / \langle x \rangle = 0.02$ and $\langle \mu_y \rangle / \langle y \rangle = 0.22$. These values are considerably better than those found in the second attempt, namely by factors 20 and 5. This gratifying result gives confidence in the data. For the gradients, $z$ and $z_0$ we found $\langle z_0 \rangle = 0.0868 \pm 0.0030$ and $\langle z \rangle = 0.0508 \pm 0.0020$. Further $\langle (z_0-z)/z_0 \rangle = 0.454 \pm 0.018$ and $(\langle z_0 \rangle - \langle z \rangle)/\langle z_0 \rangle = 0.415$. The difference between the two last numbers is satisfactorily small which implies that the involved error curves are symmetric. It allows one to derive the average of the two values, which is 0.43.

Adhering to these results of the third attempt, the *conclusions* from this section are:

The average gradient of the tropospheric temperature during the period 1619–1970 was $\langle z_0 \rangle = 0.0868 \pm 0.0030$ °C/century.

The fraction 0.43, being 0.037 °C/century was correlated with solar variability.

The average temperature gradient correlated with the toroidal field component is 0.077 °C/century, while that correlated with the poloidal field component was $-0.040$ °C/century. The minus sign of the $y$ value tells that sun-induced warming due to the poloidal field component is strongest for weakest polar fields, when coronal holes are strong while polar faculae (Callebaut

and Makarov, 1992) and bright spots virtually absent. This finding has implications for our understanding of the sun–climate connection, perhaps also in view of the sometimes advanced assumption of a relation between solar particle emission and cloud formation. One may wonder if this result has implications for the good correlation between polar and equatorial magnetic fields, but that latter correlation is just a basic aspect of the solar dynamo and not related to the present result. In Section 7 we return to it.

The residual non-solar terrestrial surface temperature gradient, hence obtained after having subtracted the solar part and presumably to be ascribed to climatologic causes is 0.051 °C/century.

We reiterate that the temperature gradients $z_0$ and $z$ are averages for the whole period 1619–1970 and that there are indications for variations with time. These variations are not discussed in this paper.

These results are to be considered as an improvement of those published in De Jager and Duhau (2009b). They replace the former results.

## 3. Episodes of global warming and cooling?

In our previous paper (De Jager and Duhau, 2009b) it was concluded that the residuals $\Delta T = T_{observed} - T_{calculated}$, from which the average increase $z$ has been subtracted, show clear residual episodes of relative warming and cooling. One of these is the present period of global warming that did not seem to differ in its various aspects from the other periods. Since that conclusion appears to oppose generally accepted views (cf. also Komen, preprint), a closer consideration is needed. We do that in the present section.

To that end we calculated $\Delta T$ for the data set of Moberg et al. (2005) to which the end part of that of Brohan et al. (2006) and Kennedy et al. (2008) are pasted. This is the same set of data that is used in Fig. 1. In view of the possible change in gradient $dT/dt$ around 1790–1800 we restrict ourselves in this section to the period after 1790, but we included the period after 1970 because we also wish to investigate that period. We based this study on the average $x$ and $y$ values listed at the end of the preceding section. The results are presented in Fig. 3.

With regard to the diagram we remark the following. Although the input data are for 1790–2008 the diagram shows them only for 1799–1999. That is because the $T$-data have been smoothed by a 19 years triangular smoothing program, which shortens the outcome by 9 years at either end of the data file. Apart from the small oscillations in the curve of Fig. 3, showing amplitudes between 0.1° and 0.2°, there is a conspicuous depression of $\sim 0.2°$ near 1960 and a stronger warming, reaching 0.30° in 1999. We identify the latter with the recent period of global warming until the end of the last century. The presently followed procedure does not allow a determination for years after 1999. On one hand a

**Table 1b**
Values of $x$, $y$, $z_0$ and $z$ along with their r.m.s. errors ($\mu$) for the seven temperature files and the two approaches (upper set: first $x$, then $y$; lower set: the reverse approach).

| T-file | x | $\mu_x$ | y | $\mu_y$ | $z_0$ | z | $\mu_z$ |
|---|---|---|---|---|---|---|---|
| 1 | .1030 | .0075 | +.1427 | .0387 | .1704 | .1103 | .0052 |
| 2 | .3179 | .0133 | −.1688 | .0697 | .0734 | .0419 | .0092 |
| 3 | .3517 | .0143 | −.2258 | .0709 | .0362 | .0112 | .0099 |
| 4 | .2078 | .0088 | −.0532 | .0493 | .0849 | .0499 | .0061 |
| 5 | .3115 | .0128 | −.1663 | .0660 | .0767 | .0460 | .0089 |
| 6 | .2388 | .0113 | −.0026 | .0540 | .1608 | .1058 | .0078 |
| 7 | .1660 | .0070 | −.0295 | .0507 | .0644 | .0336 | .0049 |
| 1 | .3553 | .0062 | −.0940 | .0251 | .1704 | .1113 | .0043 |
| 2 | .4471 | .0052 | −.2900 | .0287 | .0734 | .0424 | .0036 |
| 3 | .4529 | .0046 | −.3207 | .0259 | .0362 | .0116 | .0032 |
| 4 | .3531 | .0038 | −.1895 | .0222 | .0849 | .0505 | .0026 |
| 5 | .4370 | .0045 | −.2840 | .0262 | .0767 | .0465 | .0032 |
| 6 | .4681 | .0065 | −.2178 | .0240 | .1608 | .1067 | .0045 |
| 7 | .3438 | .0032 | −.1866 | .0255 | .0699 | .0369 | .0022 |
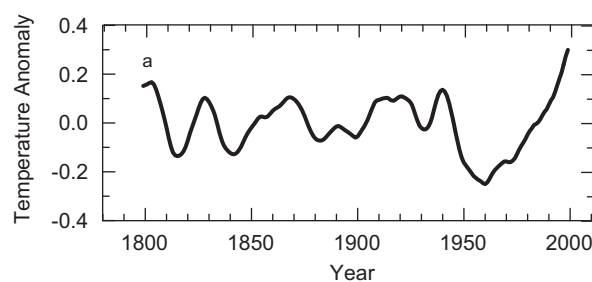


**Fig. 3.** Values of the residuals $\Delta T = T_{observed} - T_{calculated}$ for the period 1799–1999.

further increase may be expected being given that the excesses were 0.24° and 0.27° in 1997 and 1998, hence an increase of 0.03° per year. On the other hand the 1999 value is greatly influenced by the exceptional 1998 maximum, which is ascribed to strong El Niño effects.

The depression around 1960 is part of the Grand Maximum of the 20th century. A significant cooling dominated by aerosols, is a robust feature of a wide range of detection analyses. A key factor in identifying the aerosol fingerprint, and therefore the amount of aerosol cooling is the change through time of the hemispheric temperature contrast, which is affected by the different evolution of aerosol forcing in the two hemispheres as well as the greater thermal inertia of the larger ocean area in the Southern Hemisphere (Santer et al., 1995, 1996; Hegerl et al., 2001; Stott et al., 2006). Regional and seasonal aspects of the temperature response may help to distinguish the response to greenhouse gas increases from the response to aerosols (e.g., Ramanathan et al., 2005; Nagashima et al., 2006).

A final remark is appropriate at this point. For the present period of global warming we find for the year 1999 a peak value of 0.31 °C. In our previous paper (De Jager and Duhau, 2009b) we found a smaller value, ~0.2 °C. The difference reflects the present more precise analysis: the earlier study was based on an analysing method similar to the 'first attempt' as described in Section 2.

Another aspect is that the direct temperature data show a larger present-days excess; e.g. the Brohan et al. (2006) and Kennedy et al. (2008) data give a difference of ~0.7–0.8 °C between the maximum years 2005 and 2008 and the average of the years 1960–1970. A similar difference is noted by Komen (preprint) who was unable to reproduce the data from our former study. That is due to his use of other normalizing constants and to his neglect of smoothing.

The difference between the direct observations and our derived value of ~0.3 °C is for a minor part, not more than 0.1 °C, accounted for by the subtraction of the gradual increase. For another part it is related to the dip of ~0.3° around 1960–1970. The major part of the difference is due to the smoothing of the data. Data smoothing is essential if one wishes to deal with climate change instead of studying short-term variations. But this procedure especially affects steep gradients and peaks in the unsmoothed curve. Some trial calculations, applied to the present period of global warming including the standstill of the temperature increase during the last decade (Kerr, 2009) have shown that the smoothing may account for a reduction by ~0.3 to ~0.4 °C of the peak that would result from unsmoothed data. The sum of these effects explains the difference.

*Concluding* this section we summarize:

- The triangularly weighted average residual smoothed over the period 1990–2008 is 0.31°. This should be compared with an average residual of 0.15 °C in the period 1800–1950.
- In the 1960s the smoothed residual is negative (approx. −0.2°). This can, most probably, be ascribed to aerosol cooling.

## 4. Wavelet representation

In Section 5 we want to investigate the dependence of temperature on the various components of the solar fields, in order to find hints leading to a physical explanation. In order to split the various variables (temperature, poloidal and toroidal fields) in their components, we used the method of wavelet representation as introduced by Duhau and Chen (2002) and improved by Duhau and De Jager, (2008). These authors have
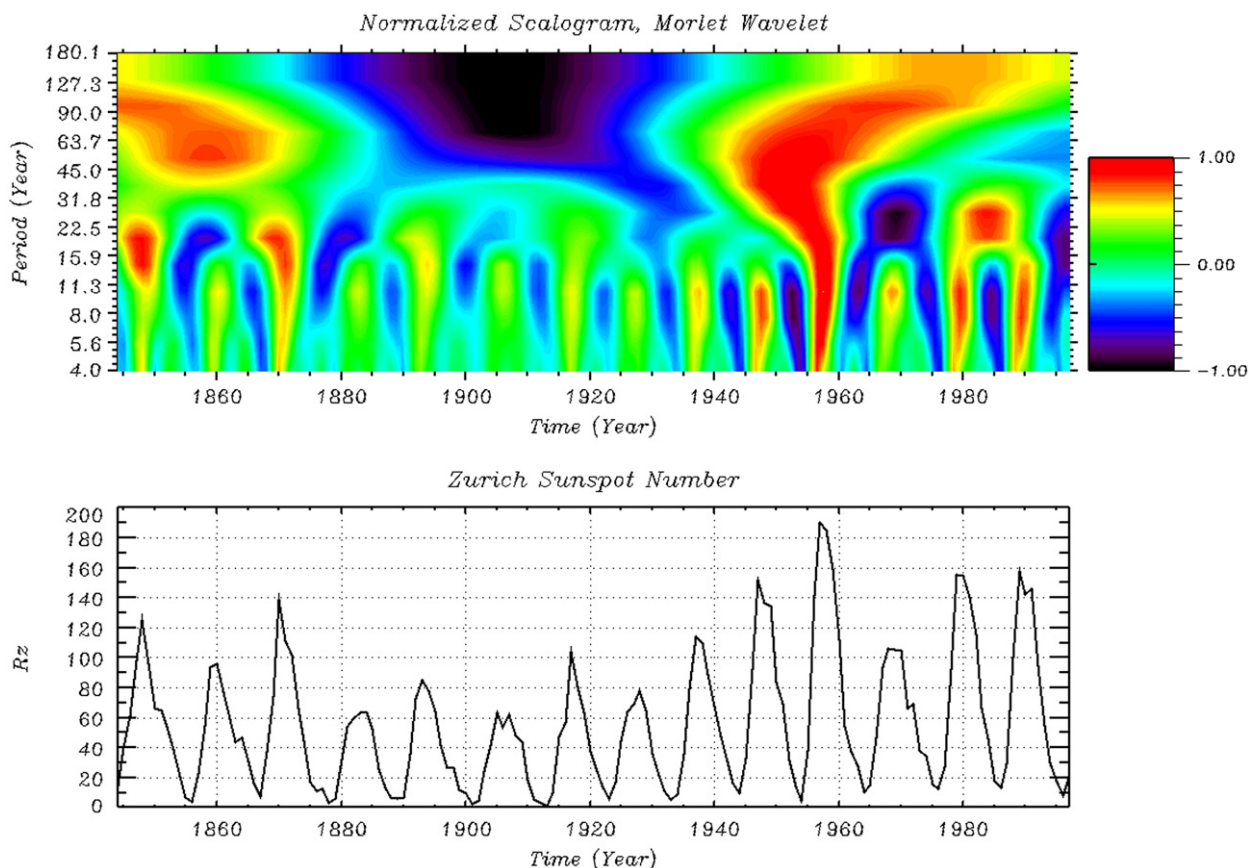


Fig. 4. The Morlet wavelet scalogram of the annual mean sunspot number for the last 150 years (copied from Duhau and Chen, 1999).

shown that the amplitude modulation of the 11 years solar magnetic field cycle oscillates around a fixed unique state, the Transition Point. As the solar dynamo, from which the solar magnetic fields originate, is a closed system, it may therefore maintain proper modes of oscillation.

Fig. 4 shows the Morlet wavelet scalogram for 150 years of sunspot number data. A given proper mode of oscillation is displayed there by a succession of dark and lighter areas occurring at quasi-regular intervals and covering a band of periods. We denominate these proper modes by the term 'cycles'. We assume that these are quasi-harmonics. In the scalogram of Fig. 4 we identify four ranges of sunspot numbers whose periods are roughly in the bands: 7–15, 15–32, 32–75 and above 75 years. We denote these by Schwabe-type, Hale-type, lower Gleissberg, upper Gleissberg and Suess (De Vries) periods.

Fig. 5 shows the time series of $R_{max}$ and $aa_{min}$ as normalized with respect to the coordinate values of the so-called Transition Point (Duhau and De Jager, 2008). The vertical co-ordinate gives the amplitudes of the poloidal and the toroidal transition cycles in sunspot number units and in nT, respectively, according to

$$r_{max} = \frac{R_{max} - tp_R}{tp_r} \qquad (2a)$$

$$AA_{min} = \frac{aa_{min} - tp_{aa}}{tp_{aa}} \qquad (2b)$$

In Fig. 5 the sunspot maxima and the geomagnetic $aa$ minima time series are extrapolated till 2009 and 2014, respectively, on the basis of the forecast by De Jager and Duhau (2009a). Note that in this diagram the time resolution of the series is 11 years, while it is 1 year in Fig. 4. Therefore, since the smallest resolvable period is twice the sample period (Torrence and Compo, 1998), the resolution is 22 years in the first case and in the second case it is 2 years. Hence, the band of sunspot numbers below ~20 years is not resolved in the time series of Fig. 5, which means that the Schwabe signal is filtered out in that time series.

Table 2 gives the Fourier periods of the wavelet components of the base functions that allow for an accurate representation of the 400 years long time series. While the lower Gleissberg band correspon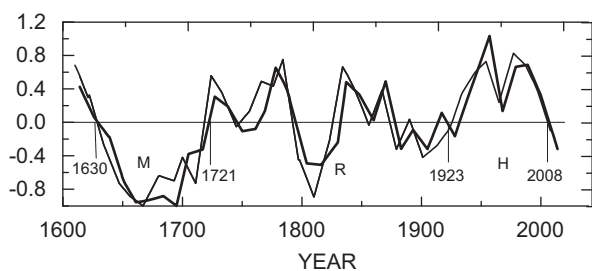ds in the solar dynamo to a semi-secular cycle, the upper Gleissberg band and above are included in the so-called Gleissberg cycle (De Jager and Duhau, in press). The parameters $D$ and $n$ that define the base functions in Table 2 are the ratios of the widths of the Gaussian envelope to the Fourier period of each wavelet component and the number of subscales between scales (see Torrence and Compo, 1998). The Fourier periods correspond to time scales that we distinguish by Hale, lower Gleissberg, upper Gleissberg and De Vries (Suess) periods in solar activity. The 'long-term' part, which contains the linear trend, is not presented in the table. With regard to the periods above ~75 years Duhau and De Jager (2008) have found that signals corresponding to different time scales in the proxy data of solar activity, based on cosmogenic isotope data, as compared with those based in sunspot number and auroral observations, differ strongly in magnitude above the 440 year period, these being strongly amplified in cosmogenic isotope data as compared with those for shorter time scales. Signals above 400 years are hard to identify in our observational time span of less that 4 centuries. In the further part of this paper we, therefore, restrict ourselves to the shortest three sets of periods, called Hale, lower Gleissberg and upper Gleissberg, because the only physically significant periodicities that have so far been identified are the Hale cycle (varying around 22 years), the Gleissberg cycle (50–140 years with a maximum at 88 years) and the sharp De Vries cycle of 205 years (De Jager, 2005).

## 5. Analysis of the components

We made the analysis for the oscillations that result from superimposing the Hale, the lower Gleissberg and the upper Gleissberg band and the above terms of Table 2, respectively. To the latter we added the linear gradual increase and we denote this complex by the term 'long-term' components.

We performed this analysis for the two main field components of the dynamo. This procedure allows one to represent the three distinctive cycles that we have identified in the solar magnetic field: the Hale, the semi-secular and the Gleissberg cycles, respectively, the last being the oscillations around the transition level as seem in the long-term component. To interpret this result we recall that the physical nature of a turbulent flow in a bound nonlinear system depends on the time and spatial scales involved. In such a system the flow is stochastic in the smallest scales. In these scales the spectrum is nearly continuous (red noise). But the large-scale organized current flows depend on the boundary condition and so this large-scale flow may sustain normal modes. As a result the spectrum of solar activity related variables (for a review see de Jager, 2005) indicates that above the 17 years period a few well defined dominant frequencies, with power well above the underground continuous noise, do exist and so we may interpret the persistence on time of these dominant frequencies as a manifestation of the existence of natural modes of oscillations in the globally bound circulation pattern. Therefore the Hale and the semi-secular cycles are due to the nonlinear interaction of the magnetic field with the large-scale fluid flow, that is with the meridional circulation and torsional oscillations (see e.g. Knobloch et al., 1998). The origin of the Gleissberg cycle, which leads to the phase transitions in the solar dynamo system, is different, the fact that the dominant period changes suddenly, nearly duplicating at Grand episodes as compared with the regular ones, indicates that the change of phase is linked to a sudden change in some of the boundary conditions, a possibility being a change in the orientation of the tachocline magnetic field with respect to the convective envelope as shown by model computations in an 'intermittent off–on dynamo' (Schmitt et al., 1996) in which the random orientation of a seed field leads to the intermittent



**Fig. 5.** The time series of maximum sunspot number $R_{max}$ (thick line) and geomagnetic index minima $aa_{min}$ as normalized by Eqs. (2a) and (2b), respectively. The short vertical lines are plotted at the years of the maxima of the polar cycles for which the phase transitions occur that leaded to new Grand Episodes viz. M (Maunder Minimum; 1630–1721) the R Episode (Regular Oscillations; 1721–1923) and the H Episode (High 20th century Maximum; 1923–2008).

**Table 2**
Wavelet Fourier periods of the various components for $D=6$, $n=3$.

| Period band | Wavelet Fourier periods (years) | | | |
|---|---|---|---|---|
| Hale | 17.00 | 21.42 | 26.98 | |
| Lower Gleissberg | 34.00 | 42.84 | 53.97 | 68.0 |
| Upper Gleissberg | 85.67 | 107.94 | 136.0 | 171.3 |
| Suess (De Vries) | 215.9 | 272.0 | 342.4 | 431.8 |

occurrence of Grand Episodes. An empirical evidence of the validity of such a kind of models and its relationship with the solar dynamo phase transitions is given by the fact that during the 1923 phase transition the solar wind has changed from northward to southward asymmetry (Mursula and Zieger, 2001).

We performed our analysis for the Moberg et al. temperatures. They do not extend beyond 1980 and so we decided to assume the Moberg et al. data up to 1850 and to pad the Brohan–Kennedy data set to it. The combined file extends up to 2008. A small adaptation subtraction was needed for correct patching. Thereafter we decomposed the $R_{max}$ file (toroidal component), the $aa_{min}$ file (poloidal) and the temperature file $T$ into the Hale, semi-secular and long-term components with the wavelet analysis technique, described in Section 4, that we also used in our earlier paper (Duhau and De Jager, 2008).

We carried the analysis out for the Hale, the lower Gleissberg and the upper Gleissberg components of Table 2. To the latter we added the quasi-linear gradual increase and we denote the complex by the long-term component. We performed this analysis for the two main field components of the dynamo.

We are searching for the fractional contributions of the three components of each of the two variables $R_{max}$ and $aa_{min}$ to the temperature and this leads to the following equations:

$$T\text{-}hale = CR1\ R\text{-}hale + Ca1\ a\text{-}ahale \tag{3a}$$

$$T\text{-}lower = CR2\ R\text{-}lower + Ca2\ aa\text{-}lower \tag{3b}$$

$$T\text{-}long = CR3\ R\text{-}long + Ca3\ aa\text{-}long \tag{3c}$$

It is our aim to determine the six constants $CR1$–$Ca3$ on the basis of observational data from the period 1844–1980. This is a short interval of time but direct observations of $aa$-data are only available after 1844. By writing

$$T\text{-}comp = constant + x R_{max} + y\ aa_{min} \tag{4}$$

we obtained three sets of $x$ ($=CR$) and $y$ ($=Ca$) values, one set for each of the components. These $x$ and $y$ values are identified with the parameters $CR1$–$Ca3$ from Eqs. (3a) through (3c). The value of the constant is physically uninteresting; it is just a zero-point value of the temperature scale. The determination of the parameters $x$ and $y$ by least-squares is straightforward.

The results *viz.* the six constants $CR1$, $CR2$, $CR3$, $Ca1$, $Ca2$ and $Ca3$ are presented in Table 3, together with their mean errors. The table also gives the r.m.s. deviation per data point of the fitting $T_{obs}$–$T_{cal}$, expressed in °C; this being another measure of the goodness of fit.

This approach is fully different from that followed in Section 2 of this paper but the results confirm our earlier conclusion (De Jager and Duhau (2009b) and Section 2 of this paper) that the contribution of the poloidal field to tropospheric temperatures is for two of the components in order of magnitude comparable to that of the toroidal field. This does not apply to the lower Gleissberg component. The fact that the $x$ value for the Hale component is negative make us doubt its reality, in view of the results found in Section 2. We note the negative signs of the $y$

components, which confirm the earlier results (Section 3). The r.m.s. deviation per data point ($\langle \mu \rangle$) is also in acceptable bounds. These results may explain why former analyses (Krivova and Solanki, 2003; Foukal et al., 2006; Erlykin et al., 2009a), that are all based on studies of the toroidal field component only, such as sunspot number data or Total Solar Irradiance data, did not give positive results for the dependence of tropospheric temperature on solar parameters.

The present analysis, and particularly the data of Table 3, gives some clues that may be helpful to guide future investigations. The essential problem is to find the physical explanation of the lower Gleissberg variations (being the superposition of wavelet components with periods in the lower Gleissberg band). This is yet an open problem. We briefly return to this item in Section 7.

It is useful also to consider the plots of the residuals $\Delta T = T_{obs} - T_{cal}$ for the three components of solar variability. They are plotted in Fig. 6 whereby in the case of the long-term component the gradual increase has been subtracted. We recall that the $x$ and $y$ values were derived from the data for the period 1844–1980. The diagrams, though, have been extended to the period from 1610 to 2008. As written before, observed $aa$-data do not exist before 1844 and we used the extrapolated $aa$-values of Nagovitsyn (2005, 2006, 2007) for the period 1610–1844, realizing, of course, that these have not the same value as direct observation. We analysed them in a previous investigation (Duhau and De Jager, 2008) and found them reasonably reliable. Pleasingly, in that longer period of time the deviations appear to be small for the two shortest components. The relative uncertainty of the $aa$-data in the earlier period and the extrapolation of the basic constants may be responsible for the larger deviations in the long-term component for the first part of the 17th century.

Apparently the average deviations from zero, $\Delta T$, is of the order of 0.1° in the period before 1980 (see also Table 3) but $\Delta T$ is larger after 1980, up to about 0.2°.

**Table 3**
Temperature dependence of components of solar variability. The 4th and 6th columns give the r.m.s. values $\mu_x$ and $\mu_y$ of the two parameters $x$ and $y$.

| Comp. | const | x | $\mu_x$ | y | $\mu_y$ | $\langle \mu \rangle$ |
|---|---|---|---|---|---|---|
| Hale | .0027 | −.105 | .049 | −.147 | .045 | .082 |
| Lower | .0082 | +.102 | .039 | −.001 | .033 | .110 |
| Long | −.841 | 1.336 | .071 | −.819 | .069 | .159 |

The last column gives the r.m.s. of the fitting of ($T_{obs}$–$T_{cal}$) in degrees centigrade. The data apply to the period 1844–1980.



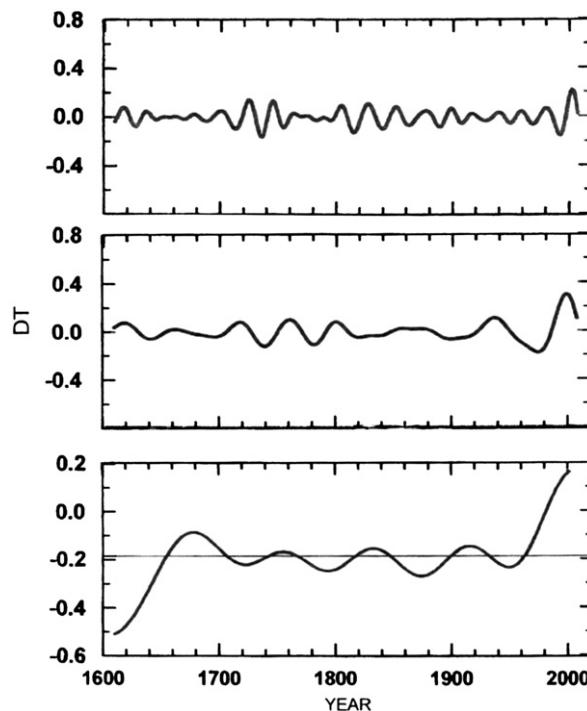**Fig. 6.** Calculated temperature residuals $\Delta T = T_{obs} - T_{cal}$ for the Hale (upper frame), the lower Gleissberg (middle frame) and the long-term components for the period 1610–2008. When comparing these diagrams one should note the different ordinate scales. The constants on which these diagrams are based were derived for the period 1844–1980. Hence, large parts of the diagrams are extrapolations.

These findings ask for identifying the physical causes of the relevant field components: the Hale and long-term components of the two fields. Finding them may appear important for understanding the mechanism of the sun–climate relationship. We deal with that problem in Section 7.

With a view to the negative signs in Tables 1a, 1b and 3 and considering Fig. 6 and the results found in Section 2, the *conclusion* of this section is that gradual tropospheric warming during the period 1790–1970 was mainly correlated with the long-term components of solar variability. The Hale and the semi-secular (lower Gleissberg) components may rather be related to the onset of new Grand Episodes through the associated torsional oscillations.

## 6. Changing solar activity and evidence for solar forcing of climate change during the Holocene

This paper deals with surface temperature variation during the period in which sufficient solar observations are available (1610–present). But there is abundant indirect evidence of solar variations corresponding to climate fluctuations throughout the Holocene. We summarize these in this section because their study may help to solve unresolved problems.

To extend the record of solar activity indirect proxy data can be derived from measurements of the cosmogenic radionuclides $^{10}$Be and $^{14}$C (radiocarbon) in natural archives such as ice cores and tree rings (Beer et al., 1990, 2006; Muscheler et al., 2004; Stuiver et al., 1991; Solanki et al., 2004; Usoskin et al., 2004b, 2004c; Beer and van Geel, 2008, Steinhilber et al., 2009). Cosmogenic radionuclides are produced continuously in the atmosphere as a result of the interaction of galactic cosmic rays with nitrogen and oxygen. The higher the cosmic ray intensity, the larger the production rate. Cosmic ray intensity is modulated by two magnetic effects: the solar activity and the geomagnetic field. Depending on the magnetic activity, the Sun emits plasma (solar wind) carrying magnetic fields into the heliosphere that acts as a shield and reduces the cosmic ray intensity. The second shielding effect is due to the geomagnetic field. After production $^{10}$Be becomes attached to aerosols and is removed from the atmosphere mainly by wet deposition within 1–2 years. Ice cores are excellent archives to measure $^{10}$Be. $^{14}$C forms $^{14}$CO$_2$ and exchanges between atmosphere, biosphere and ocean. As a consequence of the large size of these reservoirs and the long residence times the amplitude of an observed $^{14}$C change in the atmosphere is considerably smaller than the corresponding change in the production rate and the atmospheric $^{14}$C change is delayed. While the average delay is variable and can reach a century, a good average is about 20 years (Beer and van Geel, 2008). Both $^{10}$Be and $^{14}$C provide independent records of the cosmic ray intensity and solar activity of the past.

Paleoclimate reconstructions provide growing evidence for climate change. Denton and Karlén (1973) linked the radiocarbon record with geological data such as the extension of glaciers and made important conclusions about solar forcing of climate change. Magny (2004, 2007) published a long record of Holocene climate-related water table changes in lakes in south-eastern France and adjacent Switzerland. The lake level fluctuations closely correspond to the atmospheric $^{14}$C fluctuations and therefore also to the history of solar activity. Holzhauser et al. (2005) compared glacier and lake level fluctuations in west-central Europe over the last 3500 years and demonstrated synchronicity between glacier advances, periods of higher lake levels and maxima of atmospheric radiocarbon. There are numerous other examples of sediment and lake level data that point to a solar link (Baker et al., 2005; Morrill et al., 2006;

Patterson et al., 2004; Stager et al., 2005; Verschuren et al., 2000; Wu et al., 2006; Haltia-Hovi et al., 2007).

Holocene peat deposits, especially the rainwater-fed raised bogs such as those in northwest Europe, are natural archives of climate change. Climate-related changes in precipitation and temperature are reflected in the changing species composition of the peat-forming vegetation. Based on very well dated peat cores that were formed after the last Ice Age it has been shown that mire surface wetness often increased together with rapid increases of atmospheric production of $^{14}$C (Kilian et al., 1995; van der Plicht et al., 2004; van Geel et al., 1998; Speranza et al., 2003; Mauquoy et al., 2002).

The ice rafted debris found in sediment cores of the North Atlantic originates from areas in Greenland and Iceland where particles are picked up by glaciers moving towards the coast. When the ice melts in the North Atlantic the particles are released and preserved in the sediment. Their amount is therefore a measure of the transport of cooler, ice-bearing surface waters eastward from the Labrador Sea and southward from the Nordic Seas, probably accompanied by shifts to strong northerly winds north of Iceland. Bond et al. (2001) showed that more ice-rafted debris in the North Atlantic Ocean was transported to the south during periods of relatively low solar activity. The agreement between cosmogenic isotope fluctuations and ice rafted debris points to a dominant influence of solar activity changes on the North Atlantic climate.

Neff et al. (2001) studied the climate archive of stalagmites in Oman. The oxygen isotope record was interpreted as a proxy for fluctuations in monsoon rainfall. After some adjustments of the U-Th chronology, the oxygen isotope record was linked to the $\Delta^{14}$C record, suggesting that changes of monsoon intensity are driven by solar activity fluctuations. Oxygen isotopes ratios in stalagmites from the Dongge cave in southern China also show clear evidence for a solar signal in the monsoon variability on decadal to centennial time scales (Wang et al., 2005). Mangini et al. (2005) reconstructed temperature changes during the last 2000 years based on a stalagmite from a cave in the Central Alps. Based on a high correlation of that record with $\Delta^{14}$C, the conclusion was made that solar variability was a major driver of climate in Central Europe during the past two millennia. Based on measurements of $^{10}$Be in polar ice cores Steinhilber et al. (2009) presented a physics-based record of 40-year averaged total solar irradiance covering 9300 years. While the record of atmospheric $^{14}$C includes considerable system effects, such as the variable delay, the $^{10}$Be record is a more direct reflection of TSI. The reconstruction by Steinhilber et al. offers the possibility to further test links between Holocene climate fluctuations and TSI, and provides a basis for climate models to quantify the role of TSI forcing.

## 7. The solar origins of terrestrial temperature variations

The analyses of the previous sections demand for an attempt to identify the mechanisms that influence temperature variations. We need to explain the following three quantitative data:

While the total temperature increase over the period 1619–1970 was 0.087 °C/century, a gradient of 0.077 °C/century is correlated to the equatorial (toroidal) magnetic component.
A negative gradient of $-0.040$ °C/century is correlated with the poloidal component. We have to explain its value and the negative sign of the *y*-term in Eq. (1).
A gradient of 0.051 °C/century is due to other, presumably climatologic causes.

We discuss these three results:

The *equatorial (toroidal) component* of 0.077 °C/century can fully be explained by the variation of the solar radiative flux and the associated feedback by evaporated water vapour. The excess flux associated with solar equatorial activity consists of two parts: the UV flux and the component in the visual and IR part of the spectrum. Lean (2000; cf. also De Jager, 2005, Fig. 5) gives in her Fig. 9 diagrams that show the variation of these fluxes during the four centuries 1600–2000. Although direct observations of these fluxes are only available since ~1980, it is generally assumed that their variation is proportional to the number of sunspot groups, because the flux variation originates from the facular fields around the sunspot groups. This is the reason why an extrapolation of the fluxes down to 1610 on the basis of observed sunspot numbers seems allowed. From Lean's (2000) diagrams one reads a flux variation of 0.62 mW/cm$^{-2}$ nm$^{-1}$ per century. With the conventional assumption that $\Delta T/T = (\Delta I/I)/4$ one derives a tropospheric temperature variation of 0.033 °C/century. From a study by Foukal et al. (2004) we find 0.065 °C/century. From Solanki (2002) we derive 0.042 °C/century, while data from Steinhilber et al. (2009) would yield 0.014 °C/century. The straight average of these four values is 0.038 °C/century, which is 49% of the value that should be explained. This additional heating leads to water vapour evaporation which causes further heating, etc. This positive feedback by evaporated water vapour and $CO_2$ gas (Boni et al., 2006; cf. also Murphy et al., 2009) amplifies the temperature increase by a factor 2. Hence, the gratifying result of this exercise is that the gradual temperature increase that is correlated with the equatorial magnetic field component can fully be explained by the gradual increase of the Total Solar Irradiance and its feedback effects. Since the temperature increase associated with the equatorial component is thus explained there is little room left for hypothetical additional heating related to solar flares and coronal mass ejections (CMEs; Xie et al., 2009; Howard and Tappin, 2009a, 2009b; Tappin and Howard, 2009). In this connection we also refer to Soon (2009) who found that solar irradiance can explain 75% of the variance of the decadally smoothed Arctic-wide surface temperature over that past 130 years. The difference with our result asks for an explanation.

For explaining the underlying mechanism it is useful to mention that a change in the north–south asymmetry in the solar wind speed from northward to southward around 1930 was reported by Mursula and Zieger (2001). This change of symmetry may be due to a change between the spin of the outer layers of the sun and the dip direction, and, in turn, it may be related to the episode change in 1923. The possible role of torsional oscillations in explaining solar variability might be considered in this connection (Snodgrass and Howard, 1985; Vorontsov et al., 2002).

The *polar (poloidal) component* is −0.040 °C/century. As $aa_{min}$ is a measure of the strength of the poloidal field, the minus sign means that surface temperature increases when the poloidal field strength decreases, and vice versa. The maximum value of the polar field – which occurs during a sunspot minimum – may be related to the non-magnetic solar wind emanating from the coronal holes. Strong polar magnetic fields are mainly closed fields but the coronal holes, important sources for the solar wind have open field lines carrying virtually little or no magnetic fields into the heliosphere. Recent observations (Gibson et al., 2009; cf. also Savcheva et al., 2009) show that the polar solar wind reached an exceptionally high maximum during the period of extraordinary low solar polar activity of 2008–2009. At the same time the cosmic ray flux on earth reached exceptionally high values. This can be explained by the circumstances that during a solar minimum the non-magnetic solar wind component dominates, hence the solar wind carries little magnetic field into space. During a minimum of interplanetary magnetic fields, the cosmic rays flux reaches maximum values, while the differential surface temperature minimizes. This is a problem for climatology and will not be touched here. An elaborate discussion of the solar wind interaction with the Earth's environment is given by Watermann et al. (2009). Xie et al. (2009) discussed the physics of Coronal Mass Ejections near a solar minimum. Another feature that may be of importance is the coronal jets; these are always associated with the coronal bright points, which appear in positive correlation with the strength of the polar field (Nisticò et al., 2009).

The above listed components are the sources of emission of magnetized plasma and thus associated with the shielding of the earth from cosmic rays and the suggested, but not yet quantifiable, process of cloud formation (Kristjansson et al., 2004; Usoskin et al., 2004a; Svensmark et al., 2009; Ram et al., 2009, but cf. also the negative result by Sloan and Wolfendale (2008), Pierce and Adams (2009), Kulmala et al. (2009) and the indecisive results of Erlykin et al. (2009b). See also the review by Gray et al. (in press). We *conclude* that the physical interpretation of the contribution of the poloidal solar component is still open.

*Concluding* this part of the present section, we found that the temperature change related to equatorial field variations can fully be explained by the variations in the Total Solar Irradiance and the consequent feedback effects. The cooling associated with an increased polar field, able to quantitatively explain the derived temperature gradient of −0.040 °C/century, is still unexplained.

## 8. Explanation of the climatologic effects; the present global warming

We are left with the *residual component* of 0.051 °C/century. It must be ascribed to several climatologic processes: volcanic eruptions, change of atmospheric circulation patterns, etc. These processes can explain temporal terrestrial temperature variations of magnitudes comparable to or even larger than 0.05–0.1 °C. But do they also explain the *gradual* increase by 0.050° per century during the period 1620–1970? So far there is no indication of a gradual change of tropospheric conditions over the past four centuries that might explain this gradual temperature increase, but there are several studies well under way. IPCC (2007) lists 12 models that have been used to simulate the temperature variations over the last millennium. These models range from rather simple energy balance models to full global climate models and have been driven by reconstructions of volcanic forcings, solar irradiance forcing and 'other forcings'. All models are more or less successful in reproducing the observed variations (see IPCC, 2007, Fig. 6.14 on page 479). We note that these models also include a contribution by 'solar forcing', but the contribution of solar irradiance variations to temperature variations is relatively small in these models. 'Other forcings' (orbital forcing, well mixed Greenhouse gases, tropospheric sulphate aerosols, land use change, changes in ozone content, etc.) are increasingly significant from 1800 onward. Some of these models have been highly tuned and the accuracy of the reconstructed forcings is limited. Also, all models used pre-industrial solar irradiance forcings which are now thought to be too high, and the presumed high climate sensitivity to solar forcing is still a subject of active research (see e.g. Meehl et al., 2009), and models differ in their representation of other forcings. An elaborate summarizing discussion of including the influence of solar factors in climate models is by Gray et al. (in press).

Finally, the question is opportune whether the excess of 0.31° in 1999 (as compared with the reference temperature in 1960; cf. Fig. 3) is consistent with current ideas on greenhouse warming. Judging from current estimates (Ch. 9 of the 4th IPCC report) the

antropogenic part of global warming since 1960 is 0.5° with an uncertainty of 0.3°. This agrees with the result found here.

In *conclusion*, the residual temperature increase that is not correlated with solar variability (0.051 °C/century), as well as the recent residual temperature increase (0.31 °C in 1999), can both be explained by model calculations.

## 9. Conclusions

In an earlier investigation (De Jager and Duhau, 2009b) we found that the tropospheric temperatures are not only correlated with the toroidal field components of the solar dynamo, but also with variations of both the toroidal and the poloidal magnetic field components. In this paper we partly confirm that conclusion, but an important new finding is that surface temperature increases when the poloidal field strength decreases and vice versa: the influence of the poloidal component is largest for smallest fields. We find that over the period 1620–1970 the average terrestrial surface temperature slowly increased with an average gradient of 0.087 °C/century. This can be split in three parts. The first is a gradient of 0.077 °C/century that can be fully explained by the variation of the total solar irradiance and the consequent feedback by greenhouse warming due to $H_2O$ vapour.

A gradient of −0.040 °C/century is related to the poloidal field component. It is tentatively ascribed to the open (non-magnetic) solar wind flux emanating from the coronal holes; it should lead to tropospheric warming but a quantitative physical explanation is still lacking.

The residual gradient of 0.051 °C/century is correlated with climatologic processes. There are several numerical model studies which provide a quantitative explanation of secular trends but these studies differ in details and therefore further clarification is needed, particularly referring to the quantitative explanation of the found gradient.

We studied the present period of global warming and found that, in comparison to the average temperature for the period 1800–1950, it reached a value of 0.31 °C in 1999, a value that agrees with current atmospheric model calculations. Data for later years cannot be given because of the data-smoothing technique used.

We listed evidences of solar forcing of climate on longer time scales. There appears to be an increasing amount of evidence for solar forcing of climate change and associated additional warming by feedback (Bond et al., 2001; Hu et al., 2003; Maasch et al., 2005; Mauquoy et al., 2002; van der Plicht et al., 2004; van Geel et al., 1999, 2004, Versteegh, 2005;Xiao et al., 2006). We emphasize that the apparently large sensitivity of the climate system to small changes in solar activity confirms the importance of amplifying feedback processes in the climate system (Boni et al., 2006; Murphy et al., 2009).

Finally, we emphasize the importance of addressing the main open question that is left, *viz.* the explanation of the correlation of temperature change with that of the polar magnetic field component.

## Acknowledgements

## References

Baker, P.A., Fritz, S.C., Garland, J., Ekdahl, E., 2005. Holocene hydrologic variation at Lake Titicaca, Bolivia/Peru, and its relationship to North Atlantic climate variation. Journal of Quaternary Science 20, 655–662.

Beer, J., Blinov, A., Bonani, G., Finkel, R.C., Hofmann, H.J., Lehmann, B., Oeschger, H., Sigg, A., Schwander, J., Staffelbach, T., Stauffer, B., Suter, M., Wölfli, W., 1990. Use of $^{10}$Be in polar ice to trace the 11-year cycle of solar activity. Nature 347, 164–166.

Beer, J., Vonmoos, M., Muscheler, R., 2006. Solar variability over the past several millennia. Space Science Reviews 1,1. doi:10.1007/s11214-006-9047-4.

Beer, J., van Geel, B., 2008. Holocene climate change and the evidence for solar and other forcings. In: Battarbee, R.W., Binney, H.A. (Eds.), (Eds.), Natural Climate Variability and Global Warming: a Holocene Perspective. Wiley-Blackwell, pp. 138–162.

Benestadt, R.E., Schmidt, G.A., 2009. Solar trends and global warming. Journal of Geophysical Research 114, D14101.

Bond, G., Kromer, B., Beer, J., Muscheler, R., Evans, M.N., Showers, W., Hoffmann, S., Lotti-Bond, R., Hajdas, I., Bonani, G., 2001. Persistent solar influence on north Atlantic climate during the Holocene. Science 294, 2130–2136.

Boni, S., Colman, R., Kattsov, V., Allan, R.P., Bretherton, C.S., Dufresne, J.-L., Hall, A., Hallegatte, S., Holland, M.M., Ingram, W., Randall, D.A., Soden, B.J., Tselioudis, G., Webb, M.J., 2006. How well do we understand and evaluate climate change feedback processes? Journal of Climate 19 3445–3482.

Briffa, K.R., 2000. Annual climate variability in the Holocene, interpreting the message of ancient trees. Quaternary Science 19, 87–105.

Brohan, P., Kennedy, J.J., Harris, I., Tett, S.F.B., Jones, P.D., 2006. Uncertainty estimates in regional and global observed temperature changes: a new data set from 1850. Journal of Geophysical Research 111, D12106. doi:10.1029/2005JD006548.

Callebaut, D.K., Makarov, V.I., 1992. Latitude-time distribution of 3 types of magnetic field activity in the global solar cycle. Solar Physics 141, 381–390.

Coughlin, K., Tung, K.K., 2004. Eleven-years solar cycle signal in the lower atmosphere. Journal of Geophysical Research 109, D21105.

Crowley, T.J., Lowery, T.S., 2000. How warm was the Medieval warm period? Ambio 29 51–54.

De Jager, C., 2005. Solar forcing of climate. 1. Solar variability. Space Science Reviews 120, 197–241.

De Jager, C., Duhau, S., 2009a. Forecasting the parameters of sunspot cycle 24 and beyond. Journal of Atmospheric and Solar-Terrestrial Physics 71, 239–245.

De Jager, C., Duhau, S., 2009b. Episodes of residual global warming. Journal of Atmospheric and Solar-Terrestrial Physics 71, 794–798.

De Jager, C., Duhau, S., The variable solar dynamo and the forecast of solar activity; influence on terrestrial surface temperatures. In: Proceedings of the Global Warming in the 21st Century. NOVA Science Publishers, Hauppauge, NY, in press.

De Jager, C., Usoskin, I.G., 2006. On possible drivers of sun-induced climate change. Journal of Atmospheric and Solar-Terrestrial Physics 68, 2053–2060.

Denton, G.H., Karlén, W., 1973. Holocene climatic variations—their pattern and possible cause. Quaternary Research 3, 155–205.

Duhau, S., Chen, C.Y., 1999. A multi resolution wavelet analyses of the relationship between the solar sunspot number and the geomagnetic index aa. Annales AFA (Argentinean Physical Association) 11, 62.

Duhau, S., Chen, C.Y., 2002. The sudden increase of solar and geomagnetic activity after 1923 as a manifestation of a non-linear solar dynamo. Geophysical Research Letters 29 (13), 1628. doi:10.1029/2001GL013953.

Duhau, S., De Jager, C., 2008. The solar dynamo and its phase transitions during the last millennium. Solar Physics 25, 1–15.

Erlykin, A.D., Sloan, T., Wolfendale, A.W., 2009a. Solar activity and the mean global temperature. Environmental Research Letters 4, 014006.

Erlykin, A.D., Gyalai, G., Kudela, K., Sloan, T., Wolfendale, A.W., 2009b. On the correlation between cosmic ray intensity and cloud cover. Journal of Atmospheric and Solar-Terrestrial Physics 71, 1704–1806.

Feynman, J., Gabriel, S.B., 1990. Period and phase of the 88-year solar cycle and the Maunder minimum - Evidence for a chaotic sun. Solar Physics 127, 393–403.

Foukal, P., North, G., Wigley, T., 2004. A stellar view on solar variability and climate. Science 306, 68.

Foukal, P., Fröhlich, C., Spruit, H., Wigley, T.M.L., 2006. Variations of solar luminosity and their effects on Earth's climate. Nature 443, 161–166.

Gibson, S., Kozyra, J., de Toma, G., Ernory, B., Onsager, T., Thompson, B., 2009. If the Sun is so quiet, why is the Earth ringing? A comparison of two solar minimum intervals. Journal of Geophysical Research 114, A09195.

Gray, L.J., Beer, J., Geller, M., Haigh, J.D., Lockwood, M., Matthes, K., Cubasch, U., Fleitmann, D., Harrison, G., Hood, L., Luterbacher, J., Meehl, G.A., Shindell, D., Van Geel, B., White, W., Solar influence on climate. Reviews in Geophysics, in press.

Haltia-Hovi, E., Saarinen, T., Kukkonen, M., 2007. A 2000-year record of solar forcing on varved lake sediment in eastern Finland. Quaternary Science Reviews 26, 678–689.

Hegerl, G.C., Jones, P.D., Barnett, T.P., 2001. Effects of observational sampling errors on the detenction of anthropogenic climate change. Journal of Climate 14, 196–207.

Holzhauser, H., Magny, M., Zumbuhl, H.J., 2005. Glacier and lake-level variations in west-central Europe over the last 3500 years. Holocene 15, 789–801.

Howard, T.A., Tappin, S.J., 2009a. Interplanetary coronal mass ejections observed in the heliosphere; 1. Review of theory. Space Science Reviews 147, 31–54.

Howard, T.A., Tappin, S.J., 2009b. Interplanetary coronal mass ejections observed in the heliosphere; 3. Physical implication. Space Science Reviews 147, 89–110.

Hu, F.S., Kaufman, D., Yoneji, S., Nelson, D., Shemesh, A., Huang, Y., Tian, J., Bond, G., Clegg, B., Brown, T., 2003. Cyclic variation and solar forcing of Holocene climate in the Alaskan subarctic. Science 301, 1890–1893.

IPCC, 2007. Climate change, Fourth Assessment Report of the UN Intergovern-mental Panel for Climate Control. The Physical Science Basis, p. 476.

Jones, P.D., Briffa, K.R., Barnett, T.P., Tett, S.B.F., 1998a. High-reduction paleomag-netic records for the last millennium; interpretation, integration and comparison with general circulation model control-ran temperature. The Holocene 8, 455.

Jones, P.D., Briffa, K.R., Barnett, T.P., Tett, S.B., 1998b. High-reduction paleomag-netic records for the last millennium; interpretation, integration and comparison with general circulation model control-run temperature. The Holocene 8, 455.

Kennedy, J., Good, S., Titchner, H., Palmer, M., 2008. Global and regional climate in 2008. Weather 64, 288–297.

Kerr, R.A., 2009. What happened to global warming? Science 326 28.

Kilian, M.R., van der Plicht, J., van Geel, B., 1995. Dating raised bogs: new aspects of AMS $^{14}$C wiggle matching, a reservoir effect and climatic change. Quaternary Science Reviews 14, 959–966.

Knobloch, E., Tobias, S.M., Weiss, N.O., 1998. Modulation and symmetry changes in stellar dynamos. Monthly Notices of the Royal Astronomical Society 297, 1123–1138.

Komen, G., Comments on Episodes of relative global warming, by De Jager and Duhau, preprint.

Kremliovsky, M.N., 1995. Limits of predictability of solar activity. Solar Physics 159, 371–380.

Kristjansson, J.E., Kristiansen, J., Kaas, E., 2004. Solar activity, cosmic rays and clouds—an update. Advances in Space Research 34, 407–415.

Krivova, N.A., Solanki, S.K., 2003. Solar variability and global warming, a statistical comparison since 1850. Advances in Space Research 34, 351.

Kulmala, M., Riipinen, W., Nieminen, ., Hulkkonen, M., Sogacheva, F.L., Manninen, H.E., Paasonen, P., Petäjä, T., Dal Maso, M., Aalto, P.P., Viljanen, A., Usoskin, I., Vainio, R., Mirme, S., Mirme, A., Minikin, A., Petzold, A., Hõrrak, U., Plaß-Dülmer, C., Birmili, W., Kerminen, V.M., 2009. Atmospheric data over a solar cycle: no connection between galactic cosmic rays and new particle formation. Atmospheric Chemical Physics Discussions 9, 21525–21560.

Lean, J.L., 2000. Short term, direct indices of solar variability. Space Science Reviews 94, 39–51.

Le Mouël, J-L., Kossobokov, V., Courtillot, V., 2005. On long-term variations of simple geomagnetic indices and slow changes in magnetospheric currents, the emergence of anthropogenic global warming after 1990? Earth and Planetary Science Letters 232 273–286.

Le Mouël, J-L., Courtillot, V., Blanter, E., Shnirman, M., 2008. Evidence for a solar signature on 20th-century temperature data from the USA and Europe. Comptes Rendus Geoscience 340, 421–430.

Le Mouël, J-L., Blanter, E., Shnirman, M., Courtillot, V., 2009. Evidence for solar forcing in variability of temperatures and pressures in Europe. Journal of Atmospheric and Solar Terrestrial Physics 71, 1309–1321.

Lockwood, M., Whiter, D., Finch, I.D., Rouillard, A.D., Clarke, E., Hancock, B., Henwood, R., Ulich, F., Linthe, H.J., Clilverd, M.A., 2009. The long-term drift in geomagnetic activity: calibration of the aa index using data from a variety of magnetometer stations. Annals of Geophysics, submitted for publication.

Maasch, K.A., Mayewski, P.A., Rohling, E.J., Stager, J.C., Karlén, W., Meeker, L.D., Meyerson, E.A., 2005. A 2000-year context for modern climate change. Geografiska Annaler 87A, 7–15.

Magny, M., 2004. Holocene climate variability as reflected by mid-European lake—level fluctuations and its probable impact on prehistoric human settlements. Quaternary International 113, 65–79.

Magny, M., 2007. Lake level studies—West-Central Europe. In: Encyclopedia of Quaternary Studies, vol. 2, 1389–1399.

Mann, M.E., Bradley, R.J., Hughes, M.K., 1999. Northern hemisphere temperatures during the past millennium; inferences, uncertainties and limitations. Geophysical Research Letters 26, 759.

Mann, M.E., Jones, P.D., 2003. Global surface temperatures over the past two millennia. Geophysical Research Letters 30, 1820.

Mayaud, P.N., 1975. Analysis of storm sudden commencements for the years 1868–1967. Journal of Geophysical Research 80, 111–122.

Mangini, A., Spotl, C., Verdes, P., 2005. Reconstruction of temperature in the Central Alps during the past 2000 yr from a delta O-18 stalagmite record. Earth and Planetary Science Letters 235, 741–751.

Mauquoy, D., van Geel, B., Blaauw, M., van der Plicht, J., 2002. Evidence from northwest European bogs shows 'Little Ice Age' climatic changes driven by variations in solar activity. The Holocene 12, 1–6.

Meehl, G.A., Tebalsi, C., Walton, G., Easterling, D., McDaniel, L., 2009. Relative increase of record high maximum temperatures compared to record low minimum temperatures in the U.S. Geophysical Research Letters 36 (23), L23701.

Moberg, A., Sonechkin, D.M., Holmgren, K., Datsenko, N.M., Karlén, M., 2005. Highly variable Northern Hemisphere temperatures reconstructed from low- and high-resolution data. Nature 433, 613–617.

Morrill, C., Overpeck, J.T., Cole, J.E., Liu, K.B., Shen, C.M., Tang, L.Y., 2006. Holocene variations in the Asian monsoon inferred from the geochemistry of lake sediments in central Tibet. Quaternary Research 65, 232–243.

Murphy, D.M., Solomon, S., Portmann, R.W., Rosenlof, K.H., Forster, P.M., Wong, T., 2009. An observationally based energy balance for the Earth since 1950. Journal of Geophysical Research 114, D17107. doi:10.1029/2009/JD012105.

Mursula, K., Zieger, B., 2001. Long term North–South asymmetry on solar wind speed inferred by geomagnetic activity: a new type of century scale oscillation? Geophysical Research Letters 28 95–98.

Muscheler, R., Beer, J., Wagner, G., Laj, C., Kissel, C., Mazaud, A., Raisbeck, G., Yiou, F., Kubik, P.K., 2004. Changes in the carbon cycle during the last deglaciation as indicated by the comparison of $^{10}$Be and $^{14}$C records. Earth and Planetary Science Letters 219, 325–340.

Nagashima, T., Shiogama, H., Yokohata, T., Takemura, T., Crooks, S.A., Nozawa, T., 2006. Effects of carbonaceous aerosols on surface temperature in the mid twentieth century. Geophysical Research Letters 33, L04702. doi:10.1029/2005GL024887.

Nagovitsyn, Yu.A., 2005. To the description of long-term variations in the solar magnetic flux: the sunspot area index. Astronomy Letters 31, 557–562.

Nagovitsyn, Yu.A., 2006. Solar and magnetic activity on a long time scale. Reconstruction and possibilities for predictions. Astronomy Letters 32, 344–352.

Nagovitsyn, Yu.A., 2007. Solar cycle during the Maunder Minimum. Astronomy Letters 33, 340–345.

Neff, U., Burns, S., Mangini, A., Mudelsee, M., Fleitmann, D., Matter, A., 2001. Strong coherence between solar variability and the monsoon in Oman between 9 and 6 kyr ago. Nature 411, 290–293.

Nisticò, G., Bothmer, V., Patsourakos, S., Zimbardo, G., 2009. Characteristics of EUV coronal jets observed with STEREO/SECCHI. Solar Physics 259, 87–108.

Overpeck, J., Hughen, K., Hardy, D., Bradley, R., Case, R., Douglas, M., Finney, B., Gajewski, K., Jacoby, G., Jennings, A., Lamoureux, S., Lasca, A., MacDonald, G., Moore, J., Retelle, M., Smith, S., Wolfe, A., Zielinski, G., 1997. Arctic environmental change of the last four centuries. Science 278 (5341), 1251–1256.

Patterson, R.T., Prokoph, A., Chang, A., 2004. Late Holocene sedimentary response to solar and cosmic ray activity influenced climate variability in the NE Pacific. Sedimentary Geology 172, 67–84.

Pierce, J.R., Adams, P.J., 2009. Can cosmic rays affect cloud condensation nuclei by altering new particle formation rates? Geophysical Research Letters 36 L09820. doi:10.1029/2009GL037946.

Ram, M., Stolz, M.R., Tinsey, B.A., 2009. The terrestrial cosmic ray flux; its importance for climate. EOS 90, 397–408.

Ramanathan, V., Ching, C., Kim, D., Bettge, T., Buja, L., Kiwhl, T., Washimgton, W.M., Fu, Q., Sikha, D.R., Wild, M., 2005. Atmospheric brown clouds: impacts on South Asian climate and hydrological cycles. Proceedings of the National Academy of Sciences 102, 5326–5333.

Santer, B.D., Taylor, K.E., Wigley, T.M.L., Penner, J.E., Jones, P.D., Cubasch, U., 1995. Towards the detection and attribution of an anthropogenic effect on climate. Climate Dynamics 12, 77–100.

Santer, B.D., Wigley, T.M.L., Mitchell, J.B.F., Oort, A.H., Stouffer, R., 1996. A search for human influences in the thermal structure of the atmosphere. Nature 382, 39–46.

Savcheva, A., Cirtain, J., DeLuca, E.E., Golub, L., 2009. Does a polar coronal hole's flux emergence follow a Hale-like law? Astrophysical Journal Letters 702 32.

Scafetta, N., 2009. Empirical analysis of the solar contribution to global mean air surface temperature change. Journal of Atmospheric and Solar-Terrestrial Physics 71, 1916.

Schmitt, D., Schüssler, M., Ferriz-Mas, A., 1996. Intermittent solar activity by an on-off dynamo. Astronomy and Astrophysics 311, L1.

Sloan, T., Wolfendale, A.W., 2008. Testing the proposed causal link between cosmic rays and cloud cover. Environmental Research Letters 3, 024001.

Snodgrass, H.B., Howard, R., 1985. Torsional oscillations of the sun. Science 228, 945–950.

Solanki, S., 2002. Solar variability and climate change; is there a link? Astronomy and Geophysics 43 5–9.

Solanki, S.K., Usoskin, I.G., Kromer, B., Schussler, M., Beer, J., 2004. Unusual activity of the Sun during recent decades compared to the previous 11,000 years. Nature 431, 1084–1087.

Soon, W.W.H., 2009. Solar arctic-mediated climate variation on multidecadal to centennial timescales: empirical evidence, mechanistic explanation, and testable consequences. Physical Geography 30, 144–184. doi:10.2747/0272-3646.30.2.144.

Speranza, A., van Geel, B., van der Plicht, J., 2003. Evidence for solar forcing of climate change at ca. 850 cal BC from a Czech peat sequence. Global and Planetary Change 35, 51–65.

Stager, J.C., Ryves, D., Cumming, B.F., Meeker, L.D., Beer, J., 2005. Solar variability and the levels of Lake Victoria, East Africa, during the last millenium. Journal of Paleolimnology 33, 243–251.

Steinhilber, F., Beer, J., Fröhlich, C., 2009. Total solar irradiance during the Holocene. Geophysical Research Letters 36, L19704. doi:10.1029/2009GL04040142.

Stott, P.A., Joes, G.S., Lowe, J.A., Thorne, P., Durman, C., Johns, T.C., Thelen, J.-C., 2006. Transient climate simulations with the HadGEM1 climate model:

causes of past warming and future climate change. Journal of Climate 19, 2763–2782.

Stuiver, M., Braziunas, T.F., Becker, B., Kromer, B., 1991. Climatic, solar, oceanic and geomagnetic influences on Late-Glacial and Holocene atmospheric $^{14}C/^{12}C$ change. Quaternary Research 35, 1–24.

Svensmark, H., Torsten, B., Svensmark, J., 2009. Cosmic ray decreases affect atmospheric aerosols and clouds. Geophysical Research Letters 36, L15101.

Tappin, S.J., Howard, T.A., 2009. Interplanetary coronal mass ejections observed in the heliosphere; 2. Model and data comparison. Space Science Reviews 147, 31–54.

Torrence, C., Compo, G.P., 1998. A practical guide to wavelet analysis. Bulletin of the American Meteorological Society 79, 61–78.

Usoskin, I.G., Marsh, N., Kovaltsov, G.A., Mursula, K., Gladysheva, O.G., 2004a. Latitudinal dependence of low cloud ionisation on cosmic rays induced ionisation. Geophysical Research Letters 31, L16109. doi:10.1029/2004GL019507.

Usoskin, I.G., Schüssler, M., Solanki, S.K., Mursula, K., 2004b. Solar activity over the last 1150 years: does I correlate with climate? In: Favata, F., Hussain, G., Battrick, B., (Eds.), 13th Cool Stars Workshop, pp. 19–22.

Usoskin, I.G., Solanki, S.K., Schüssler, M., Mursula, K., Alanko, K., 2004c. Reconstruction of solar activity for the last millennium using $^{10}Be$ data. Astronomy and Astrophysics 413, 745.

Usoskin, I.G., Mironova, I.A., Korte, M., Kovaltsov, G.A., Regional millenial trend in the cosmic ray induced ionisation of the troposphere. Journal of Atmospheric and Solar-Terrestrial Physics, in press.

van der Plicht, J., van Geel, B., Bohncke, S.J.P., Bos, J.A.A., Blaauw, M., Speranza, A.O.M., Muscheler, R., Bjorck, S., 2004. The Preboreal climate reversal and a subsequent solar-forced climate shift. Journal of Quaternary Science 19, 263–269.

van Geel, B., Bokovenko, N.A., Burova, N.D., Chugunov, K.V., Dergachev, V.A., Dirksen, V.G., Kulkova, M., Nagler, A., Parzinger, H., van der Plicht, J., Vasiliev, S.S., Zaitseva, G.I., 2004. Climate change and the expansion of the Scythian culture after 850 BC: a hypothesis. Journal of Archaeological Science 31, 1735–1742.

van Geel, B., Raspopov, O.M., Renssen, H., van der Plicht, J., Dergachev, V.A., Meijer, H.A.J., 1999. The role of solar forcing upon climate change. Quaternary Science Reviews 18, 331–338.

van Geel, B., van der Plicht, J., Kilian, M.R., Klaver, E.R., Kouwenberg, J.H.M., Renssen, H., Reyneau-Farrera, I., Waterbolk, H.T., 1998. The sharp rise of $\Delta^{14}C$ ca. 800 cal BC: possible causes, related climatic teleconnections and the impact on human environments. Radiocarbon 40, 535–550.

Verschuren, D., Laird, K.R., Cumming, B.F., 2000. Rainfall and drought in equatorial East Africa during the past 1100 years. Nature 403, 410–414.

Versteegh, G.J.M., 2005. Solar forcing of climate: evidence from the past. Space Science Reviews 120, 243–286.

Vorontsov, S.V., Christensen-Dalsgaard, J., Schou, J., Strakhov, V.N., Thompson, M.J., 2002. Helioseismic measurements of solar torsional oscillations. Science 296, 101–103.

Wang, Y.J., Cheng, H., Edwards, R.L., He, Y.Q., Kong, X.G., An, Z.S., Wu, J.Y., Kelly, M.J., Dykoski, C.A., Li, X.D., 2005. The Holocene Asian monsoon: links to solar changes and North Atlantic climate. Science 308, 854–857.

Watermann, J., Wintoft, P., Sanahuja, B., Saiz, E., Poedts, S., Palmroth, M., Milillo, A., Metallinou, F-A., Jacobs, C., Ganushkina, N.Y., Daglis, I.A., Cid, C., Cerrato, Y., Balasis, G., Aylward, A.D., Aran, A., 2009. Models of solar wind structures and their interaction with the Earth's space environment. Space Science Reviews 147, 233–270. doi:10.1007/s11214-009-9494-9.

Weiss, N.O., 1987. Dynamo processes in stars. Astrophysics Space Science Library 156, 11–29.

Weiss, N.O., Tobias, S.M., 2006. Physical causes of solar activity. Space Science Reviews 94, 99–112.

Wu, Y.H., Lucke, A., Jin, Z.D., Wang, S.M., Schleser, G.H., Battarbee, R.W., Xia, W.L., 2006. Holocene climate development on the central Tibetan plateau: a sedimentary record from Cuoe Lake. Palaeogeography, Palaeoclimatology, Palaeoecology 234, 328–340.

Xiao, S., Li, A., Liu, J.P., Chen, M., Xie, Q., Jiang, F., Li, T., Xiang, R., Chen, Z., 2006. Coherence between solar activity and the East Asian winter monsoon variability in the past 8000 years from Yangtze River-derived mud in the East China Sea. Palaeogeography, Palaeoclimatology, Palaeoecology 237, 293–304.

Xie, H., St.Cyr, O.C., Gopalswamy, N., Yashiro, S., Krall, J., Kraamar, M., Davila, J., 2009. On the origin, 3D structure and dynamic evolution of CME's near solar minimum. Solar Physics 259, 143–161.